

Homogeneous vs. realistic heterogeneous material-properties in subduction zone models: Coseismic and postseismic deformation

T. Masterlark¹, C. DeMets², H.F. Wang², O. Sanchez³, and J. Stock⁴

¹US Geological Survey, EROS Data Center, Raytheon, Sioux Falls, SD 57198; masterlark@usgs.gov

²University of Wisconsin-Madison, Madison, WI 53706; chuck@geology.wisc.edu, wang@geology.wisc.edu

³Instituto de Geofísica, UNAM, México D. F., México; osvaldo@ollin.igeofcu.unam.mx

⁴California Institute of Technology, Pasadena, CA 91125; jstock@gps.caltech.edu

1 Introduction

Three-dimensional finite-element models (FEMs) are capable of simulating tectonic deformation during all phases of the seismic cycle because they allow for heterogeneous material property distributions, complicated boundary condition and loading specifications, and contact surface interactions. These models require a dislocation source to drive the coseismic response and the subsequent poroelastic and viscoelastic relaxation.

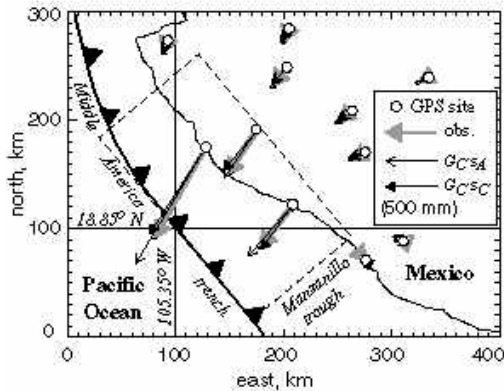


Figure 1. Coseismic horizontal GPS displacements for the 1995 ($M_w=8.0$) Colima-Jalisco earthquake. The rupture surface intersects the Middle America trench and dips to the northeast. The dashed rectangle is the surface projection of the rupture. Predictions from G_C loaded with s_A significantly overestimate the deformation magnitudes of the coastal sites. G_{CSA} and G_{CSC} are described in the text.

suggest that the seismic moment release was concentrated in two regions, one near the northwest edge of the Manzanillo trough and the other 80-120 km farther northwest [Melbourne *et al.*, 1997, Hutton *et al.*, 2001], in accord with seismologic results [Mendoza and Hartzel, 1999].

2 Assumptions and Techniques: FEM

FEMs in this study were constructed with *ABAQUS* [HKS, Inc., 2000], a commercial finite-element code that allows for poroelastic and viscoelastic material properties and contact surface interactions. A three-dimensional FEM was designed to simulate the subduction zone along the Middle America trench (Figure 2). The 28-km-thick continental crust [Pardo and Suarez, 1995] of the North American plate consists of a 16-km-thick poroelastic upper crust overlying a 12-km-thick linear viscoelastic lower crust. The oceanic crust of the Rivera plate is assumed to be 6 km thick. Poroelastic effects are neglected in the oceanic crust because they are poorly constrained by the lack of

Analytical solutions to compute Green's functions for displacement due to a dislocation are readily available [e.g., Okada, 1992]. These solutions, which include homogeneous elastic half-space (HEHS) assumptions, are often used in inverse methods to solve for dislocation distributions based on observed coseismic deformation. Alternative methods for generating displacement Green's functions, allowing for heterogeneous material property distributions, require half-space boundary conditions [Du *et al.*, 1997; Savage, 1998].

Using the 1995 Colima-Jalisco earthquake as an example, we compute FEM-generated Green's functions for both drained and undrained HEHS models and for a system with spatially varying material properties characteristic of a subduction zone. Dislocation distributions are estimated from inversion of GPS displacements. We then estimate coseismic and postseismic deformation prediction errors introduced by homogeneous material property assumptions and the sensitivity to drained versus undrained conditions.

The 9 October 1995 ($M_w=8.0$) Colima-Jalisco earthquake, which ruptured the Rivera-North American plate subduction interface (Figure 1), was the first significant rupture of the Middle America trench northwest of the Manzanillo trough since the 3 June 1932 ($M_w=8.2$) and 18 June 1932 ($M_w=7.8$) earthquakes [Singh *et al.*, 1985].

Inversions, with HEHS model assumptions, of three-dimensional coseismic displacements from 11 nearby GPS sites

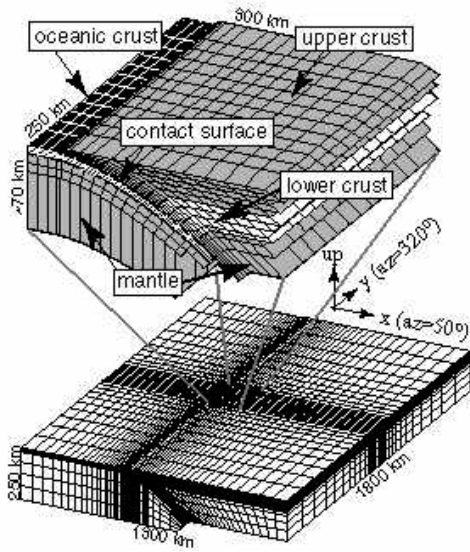


Figure 2. FEM configuration, FEM_C . The problem domain is tessellated into 24,750 three-dimensional elements. The expanded ~70 km-thick portion of the near-field region displays the heterogeneous material property distribution and subduction zone geometry. The continental lithosphere is separated into poroelastic upper crust, viscoelastic lower crust, and elastic upper mantle layers. The oceanic lithosphere includes the elastic crust overlying the elastic upper mantle. Boundary and initial conditions are discussed in the text.

fluids can flow [Wang, 2000].

The forward solution for displacements due to a dislocation distribution in an elastic material is a linear system of equations $\mathbf{G} \mathbf{s} = \mathbf{d}$ for an *a priori* fault geometry, where \mathbf{G} is the matrix of displacement Green's functions, \mathbf{s} is a vector of dislocations for contact-node pairs, and \mathbf{d} is a vector of displacements. Symbolically, the coefficient G_{ij} is a displacement component at location j due to a unit dislocation of contact-node pair i . For the case of the 1995 Colima-Jalisco earthquake, we consider reverse-slip only [Melbourne et al., 1997, Hutton et al., 2001].

Table 1. Weighted least-squares misfit

Model	Configuration	χ^2
Hutton et al. [2000]	drained HEHS	166
$\mathbf{G}_A \mathbf{s}_A$	drained HEHS	171
$\mathbf{G}_B \mathbf{s}_B$	undrained HEHS	171
$\mathbf{G}_C \mathbf{s}_C$	undrained heterogeneous	164
$\mathbf{G}_C \mathbf{s}_A$	inconsistent load	9000
$\mathbf{G}_C \mathbf{s}_B$	inconsistent load	8000

which are used to obtain dislocation distributions \mathbf{s}_A , \mathbf{s}_B , and \mathbf{s}_C respectively (Figure 3). The weighted least-squares misfits, χ^2 , from the three models are similar to those determined by Hutton et al. [2001] (Table 1).

Dislocation magnitudes determined for an undrained material will be lower than for a drained material because undrained material properties are stiffer than their drained counterparts. The heterogeneous model (FEM_C), which simulates slip along the deformable interface between oceanic and continental crust, is the stiffest of the three cases we

offshore GPS displacements. The upper mantle extends from the base of the crust in both plates to a depth of about 200 km and is treated as an elastic material. Zero displacement is specified along the lateral boundaries and base of the problem domain. The top of the problem domain is an elastic free surface. The boundaries of the poroelastic upper crust are no-flow surfaces.

Parameters chosen are as follows: poroelastic and drained elastic properties for Westerly Granite [Wang, 2000] are used for the poroelastic upper crust and viscoelastic lower crust layers respectively. The bulk hydraulic diffusivity of the upper crust is $10^{-2} \text{m}^2 \cdot \text{s}^{-1}$ [Nur and Walder, 1992; Masterlark, 2000] and the lower crust viscosity is $5 \times 10^{18} \text{Pa} \cdot \text{s}$ [Deng et al., 1998; Masterlark, 2000]. We use typical elastic properties for oceanic crust and mantle rock [Turcotte and Schubert, 1982].

The fault is a convex, deformable contact surface divided into subfaults that measure 20×10 km along-strike and down-dip respectively [Hutton et al, 2001]. Contact-node pairs are located at the center of each patch and along the top edge of the fault patches that intersect the free surface. The two lithospheric plates are welded together along the down-dip and along-strike extensions of the seismogenic portion of the interface. Initial stress and fluid-pressure conditions are geostatic.

The three mechanical systems considered are FEM_A : drained HEHS, FEM_B : undrained HEHS, and FEM_C : a heterogeneous material property distribution and poroelastic upper crust. For the two HEHS models, upper crust material properties are specified throughout the system. Drained conditions imply fluid-pressure does not change, a condition assumed in the vast majority of studies of active faults including previous solutions for dislocation distributions of the 1995 Colima-Jalisco earthquake [Melbourne et al., 1997; Mendoza and Hartzel, 1999; Hutton et al., 2001]. Undrained conditions exist in the poroelastic upper crust immediately after a sudden dislocation because stress is transferred throughout the system much faster than

We inverted the 11 measured three-dimensional coseismic displacements from Hutton et al. [2001] to obtain the mixed-determined solution for \mathbf{s} using damped least-squares methods. A weighting matrix is applied to the data vector to account for uncertainties [Menke, 1989]. Models FEM_A , FEM_B , and FEM_C generate \mathbf{G}_A , \mathbf{G}_B , and \mathbf{G}_C ,

considered due to the undrained upper crust and oceanic crust and mantle properties. Predicted seismic moments are 6.9 , 6.7 , and $6.5 \times 10^{20} \text{N}\cdot\text{m}$ for s_A , s_B , and s_C respectively, near the mid-point of seismologic estimates.

3 Results

3.1 Coseismic Predictions

There are substantial differences between coseismic predictions from FEM_C , loaded with s_C (the appropriate load) and either s_A (Figure 1) or s_B . Predictions from both s_A and s_B but using the coefficient matrix G_C overestimate displacements for the coastal GPS sites by as much as 250 mm, much more than the ~ 6 mm displacement uncertainty. Weighted least-squares misfits from these two models are more than an order of magnitude larger than for displacements predicted by s_C and using G_C (Table 1). These differences are expected based on the inconsistency between the model used to obtain the dislocation distribution and the one used to predict the displacements. These differences are also found in previous studies that used numerical methods to estimate the importance of heterogeneity on coseismic deformation predictions [e.g., *Eberhart-Phillips and Stuart, 1992; Wald and Graves, 2001*].

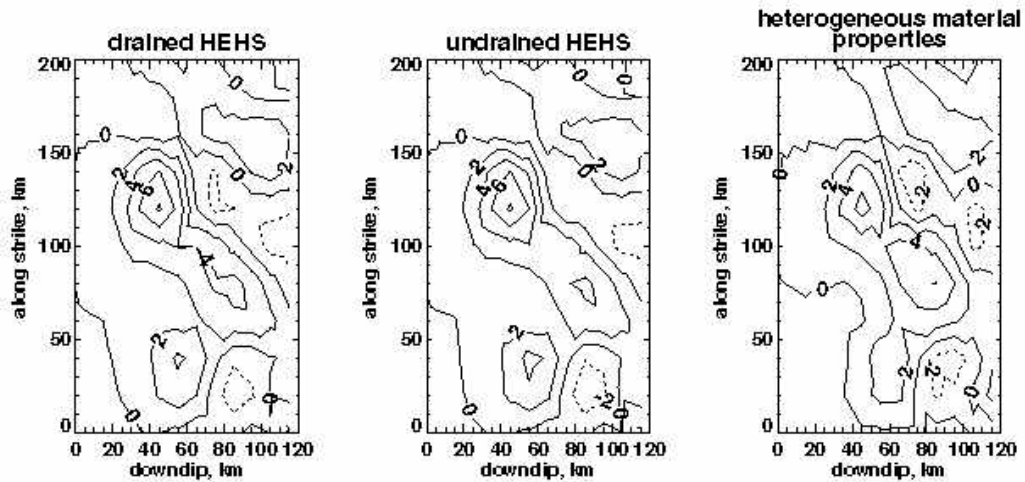


Figure 3. Coseismic dislocation distributions. The magnitudes of predicted reverse-slip dislocation along the rupture are shown for dislocation distributions s_A , s_B , and s_C respectively. The contour interval is 2 meters. Although the distributions are similar, they are not interchangeable among the models from which they were derived. The predicted seismic moment for s_A (derived from the drained HEHS model) overestimates the seismic moment of s_C (derived from the undrained model with heterogeneous material properties) by about 6 percent.

3.2 Postseismic Predictions

The coseismic response of the model to the dislocation load represents the initial conditions for the postseismic model. Fluid-pressure in the upper crust and shear stress in the lower crust, initiated by fault slip, drive poroelastic and viscoelastic relaxation. For a time step of 5 years after the earthquake, which allows for both poroelastic and viscoelastic relaxation contributions, FEM_C loaded with s_C predicts a horizontal displacement pattern of convergence toward the rupture and subsidence nearly everywhere onshore [*Masterlark et al., 2001*].

Differences between postseismic horizontal displacements predicted by FEM_C , loaded with s_C versus s_A , can be more than an order of magnitude greater than typical uncertainties (~ 6 mm) in GPS displacements. Although differences in vertical predictions are similar in magnitude, the uncertainties in vertical GPS displacements are much higher (~ 15 mm). The root-mean-squared-error in postseismic predictions, with respect to FEM_C loaded with s_C , for locations corresponding to the 11 GPS sites is 6 mm and 5 mm for FEM_C loaded with s_A and s_B respectively. The comparisons thus far represent the sensitivity to heterogeneous material properties.

The two homogeneous FEMs and their dislocation distributions are used to estimate sensitivity to poroelastic effects. The prediction difference between the initially undrained HEHS (FEM_B), loaded with s_B versus s_A , approximates the error introduced by using a dislocation distribution, determined for a drained condition assumption, in

a model that includes an undrained condition assumption. In this case, the maximum differences in the postseismic horizontal and vertical displacements are 18 mm and 13 mm respectively. The horizontal differences exceed the uncertainties in the GPS displacements. The dislocation distributions derived from HEHS models that assume drained conditions should thus not be used to drive models of postseismic poroelastic deformation [Bosl and Nur, 1998; Peltzer et al., 1998; Masterlark, 2000].

4 Conclusions

For the 1995 Colima-Jalisco $M_w=8.0$ earthquake, the errors introduced in both coseismic and postseismic deformation predictions by including HEHS assumptions exceed by an order of magnitude the estimated uncertainties in the GPS displacements. HEHS assumptions are unnecessary, except for simple first-order approximations, because FEM-generated Green's functions allow for realistic heterogeneous material property distributions, complicated boundary condition and loading specifications, and contact surface interactions. Furthermore, the method we propose allows for additional complexities within the capability of FEM methods. For example, material property anisotropy and topographic effects could be included in the FEM-generated Green's functions.

Results of this study are particularly relevant to seismic hazard assessments. Quantitative earthquake coupling analyses require realistic models and assumptions [Masterlark and Wang, 2000]. Transient deformational models can be used to quantify the evolution of quasi-static Mohr-Coulomb frictional states along faults [Masterlark, 2000]. Because these transient models are calibrated to observed displacements, errors introduced from HEHS assumptions should be avoided.

References

- Bosl, W., and A. Nur, Numerical Simulation of Postseismic Deformation due to Pore Fluid Diffusion, in *Poromechanics*, Edited by J.-F. Thimus, Y. Abousleiman, A.H.-D. Cheng, O. Coussy, and E. Detournay, pp. 23-28, Balkema, Rotterdam, 1998.
- Deng, J., M. Gurnis, H. Kanamori, and E. Hauksson, Viscoelastic Flow in the Lower Crust after the 1992 Landers, California, Earthquake, *Science*, 282, 1601-1772, 1998.
- Du., Y., P. Segall, and H. Gao, Quasi-Static Dislocations in Three-Dimensional Inhomogeneous Media, *Geophys. Res. Lett.*, 24, 2347-2350, 1997.
- Eberhart-Phillips, D., and W.D. Stuart, Material Heterogeneity Simplifies the Picture: Loma Prieta, *Bull. Seism. Soc.*, 82, 1964-1968, 1992.
- Hutton, W., C. DeMets, O. Sanchez, G. Suarez, and J. Stock, Slip Kinematics and Dynamics During and After the 9 October 1995 $M_w=8.0$ Colima-Jalisco Earthquake, Mexico, from GPS Geodetic Constraints, *Geophys. Jour. Int.*, accepted for publication, 2001.
- Masterlark, T.L., Regional Fault Mechanics Following the 1992 Landers Earthquake, Ph.D. Thesis, 83 pp., University of Wisconsin-Madison, Madison, Wisconsin, 2000.
- Masterlark, T., and H.F. Wang, Poroelastic Coupling Between the 1992 Landers and Big Bear Earthquakes, *Geophys. Res. Lett.*, 27, 3647-3650, 2000.
- Masterlark, T., C. DeMets, H.F. Wang, O. Sanchez, and J. Stock, Homogeneous vs. heterogeneous subduction zone models: Coseismic and postseismic deformation, *Geophys. Res. Lett.*, accepted for publication, August 2001.
- Melbourne, T., I. Carmichael, C. DeMets, K. Hudnut, O. Sanchez, J. Stock, G. Suarez, and F. Webb, The Geodetic Signature of the $M_{8.0}$ Oct. 9, 1995, Jalisco Subduction Earthquake, *Geophys. Res. Lett.*, 24, 715-718, 1997.
- Mendoza, C., and S. Hartzell, Fault-Slip Distribution of the 1995 Colima-Jalisco, Mexico, Earthquake, *Bull. Seism. Soc.*, 89, 1338-1344, 1999.
- Menke, W., *Geophysical Data Analysis: Discrete Inverse Theory*, 289 pp., Academic Press Inc., San Diego, Calif., 1989.
- Nur, A. and J. Walder, Hydraulic Pulses in the Earth's Crust, in *Fault Mechanics and Transport Properties of Rocks*, Edited by B. Evans and T.F. Wong, pp. 461-473, Academic Press, London, 1992.
- Okada, Y., Internal Deformation due to Shear and Tensile Faults in a Half-Space, *Bull. Seism. Soc.*, 82, 1018-1040, 1992.
- Pardo, M., and Suarez, Shape of the Subducted Rivera Plate in Southern Mexico: Seismic and Tectonic Implications, *J. Geophys. Res.*, 100, 12357-12373, 1995.
- Peltzer, G., P. Rosen, F. Rogez, and K. Hudnut, Postseismic Rebound Along the Landers 1992 Earthquake Surface Rupture, *J. Geophys. Res.*, 103, 30131-30145, 1998.
- Savage, J.C., Displacement field for an edge dislocation in a layered half-space, *J. Geophys. Res.*, 103, 2439-2446,

1998.

Singh, S. K., L. Ponce, and S.P. Nishenko, The Great Jalisco, Mexico, Earthquakes of 1932: Subduction of the Rivera Plate, *Bull. Seismol. Soc. Am.*, 75, 1301-1313, 1985.

Turcotte, D.L., and G.J. Schubert, *Geodynamics*, 450 pp., John Wiley & Sons, New York, 1982.

Wald, D.J., and R.W. Graves, Resolution Analysis of Finite Fault Source Inversion using One- and Three-Dimensional Green's Functions 2. Combining Seismic and Geodetic Data, *J. Geophys. Res.*, 106, 8767-8788, 2001.

Wang, H.F., *Theory of Linear Poroelasticity: with Applications to Geomechanics and Hydrogeology*, 287 pp., Princeton University Press, Princeton, New Jersey, 2000.